

#### Article Info

Received: 25 Jan 2017 | Revised Submission: 20 Feb 2017 | Accepted: 28 Feb 2017 | Available Online: 15 Jun 2017

### Mechanical and Micro structural Effect of Ultrasonic Welding: Review

Abhishek Rajput<sup>\*</sup>, Arun Panchal<sup>\*\*</sup>, Ravi Butola<sup>\*\*\*</sup> and Jitendra Kumar<sup>\*\*\*\*</sup>

#### ABSTRACT

*Different aspects of Ultrasonic welding is studied, ultrasonic spot welding is widely used under special cases of dissimilar elements, it is a much more efficient, less time consuming and an alternate for Friction stir spot welding(FSSW), ultrasonic spot welded joints are studied for different aspects. Thermal measurements at the interface of ultrasonic spot welding is studied, mechanical performance and grain structure is studied with EBSD examinations. Mechanical properties of Ultrasonicassisted underwater wet welding joints are studied such as bending testing and hardness distribution. Ultrasonic spot welding of Mg alloys and Tin-alloys and temperature measurement at weld interface. A series of ultrasonic spot welding experiments of Mg alloys are studied for weld quality, weld strength and fracture morphologies. A review is done on these following observations studied on Ultrasonic Welding and its various aspects.*

**Keywords:** *Ultrasonic Assisted Underwater Wet Welding; Ultrasonic Spot Welding; Aluminium Alloy; Mechanical Properties; Bending Angle.*

#### 1.0 Introduction

In today's era of cost cutting and being responsible for environmental hazard there's an urgent need to switch to more reliable and efficient system which results in low consumption of fuel and energy. One of the simplest method to achieve this is to increase the power to weight ratio of everything moving around be it transport system or automotive and aerospace industries existing. High Power to weight ratio can also be achieved by keeping the power constant and reducing the weight considerably. This brings the urge to use light weight metals like Aluminum, Copper alloys with steel, reinforced carbon fibre, Metal Matrix composites which are light in weight without compromising the strength required.

To expand the use of these light weight alternatives while manufacturing, lower-cost joining methods are important especially with dissimilar joining capability.likewise Resistance spot welding is a used in metal joining process for steel sheet body structures, it is a result of its simplicity and low cost

of operation. However, resistance spot welding of light alloys is still problematic because of unstable weld quality, very large electrical power requirement and short electrode life. It is noteworthy that this technique requires as much as 50–100 kJ energy to perform a spot weld.

Mechanical joining, adhesive bonding, thermo mechanical joining, and fusion welding technologies have been recognized as alternatives. However, mechanical joining such as self-pierce riveting increases the weight of the body structure in addition to surface treatment costs. Furthermore, fusion welding techniques are limited by the high level of distortion and poor weldability which are characteristic of light alloys such as aluminium

Thermo mechanical joining such as friction stir spot welding was found to be a more energy-efficient technique since it is carried out in solid state, thus offering considerable potential for joining aluminium and magnesium alloys . However, the process cycle can be significantly long. Ultrasonic spot welding has received less interest in contrast to friction stir spot welding or resistance welding spot technologies. The

<sup>\*</sup>GB Pant Government Engineering College, Okhla Industrial Estate, Okhla Phase III, New Delhi, Delhi 110020

<sup>\*\*</sup>Corresponding Author: Department of Mechanical Engineering Delhi Technological University, Delhi India 110042  
(E-mail: arunpanchal23@gmail.com)

<sup>\*\*\*</sup>GB Pant Government Engineering College, Okhla Industrial Estate, Okhla Phase III, New Delhi, Delhi 110020

<sup>\*\*\*\*</sup>GB Pant Government Engineering College, Okhla Industrial Estate, Okhla Phase III, New Delhi, Delhi 110020

use of low power welding techniques has been dominant for electronics applications where welding of thin foils is common practice, but joining of thicker gauges has only recently become possible owing to the development of high power systems. HPUSW is an attractive solution for joining light materials whilst overcoming issues caused by fusion welding processes. It is also more energy-efficient, in contrast to resistance spot welding, using only 0.5–4.0 kJ per joint. Furthermore, it is even more efficient than friction stir spot welding since the energy input is dissipated along the bond line rather than the workpiece top surface. In addition, an ultrasonic weld is completed in considerably shorter welding time, giving acceptable mechanical properties and narrow heat affected zone (HAZ) damage [1].

USW technique induces the rubbing of two metal sheets by maintaining the solid state without melting, which leads to the breaking of oxide layers between contacting surfaces, producing localized heat to soften the material at the weld interface, and eventually resulting in local adhesion and formation of microwelds. It is considered as an emerging and promising technique for joining non-ferrous metals and alloys with relatively a lower melting point as well as welding dissimilar material combinations as diverse as metal/ ceramic, metal/glass, Al/Cu, and Al/steel. Some important factors have to be taken under consideration such as the operating cost, cycle time, reliability, and weld quality to able to successfully join dissimilar metals. One of the most critical issues during USW is to control the intermetallic compounds (IMCs) that form at the weld interface via a rapid diffusion process. It is reported that IMCs are brittle and a continuous IMC interface layer severely compromises the joints strength [2]

## 2.0 Literature Review

High power ultrasonic spot welding (HPUSW) is a joining technique which is performed within microseconds and can be used as an energy-efficient alternate to friction stir spot welding (FSSW). In this work [1], dynamic recrystallization and grain growth were examined using electron back scatter diffraction (EBSD). In HPUSW the temperature rises to 440°C and causes extensive deformation within the weld zone. An ultra-fine grain structure was observed in a thin band of flat weld interface. With increasing

welding time the interface was displaced and ‘folds’ or ‘crests’ appeared together with shear bands. The weld interface progressively changed from flat to sinusoidal and eventually to a convoluted wave-like pattern when the tool fully penetrated the workpiece, having a wavelength of ~1mm. Finally, the microstructure and texture varied significantly depending on the location within the weld. Although the texture near the weld interface was relatively weak, a shift was observed with increasing welding time from an initially Cube-dominated texture to one where the typical  $\beta$ -fibre Brass component prevailed.[1]

In Two dissimilar ultrasonic spot welded joints of aluminum to commercial steel sheets at different levels of welding energy were investigated. The tensile lap shear tests were conducted to evaluate the failure strength in relation to micro structural changes. The main intermetallics at the weld interface in both joints was  $\theta$  (FeAl<sub>3</sub>), along with  $\eta$  (Fe<sub>2</sub>Al<sub>5</sub>) phase in Al-to-AISI304 stainless steel joint and Fe<sub>3</sub>Al phase in Al-to-ASTMA36 steel joint, respectively. The welding strength of Al-to-AISI304 stainless steel weld samples was slightly higher than Al-to-ASTMA36 steel weld samples, whereas the fracture energies of Al-to-AISI 304 stainless steel weld samples were significantly higher as compared with Al-to-ASTMA36 steel weld samples. The welding strength of both Al-to-Steel welds were higher than other reported dissimilar USW joints in literature. The fracture surfaces of both weld joints exhibits the growth of IMC layer with increasing welding energy or time, whose inherent brittleness compromises the integrity of joints. In both cases, the lap shear tensile fracture occurred from the Al/Fe interface at lower energy inputs and the failure mode at higher welding energy inputs became the “transverse through-thickness crack growth” at the edge of the nugget zone on the softer Al side.[2]

The Ultrasonic assisted underwater wet welding process (U-FCAW) results in high performance welding joints. The addition of ultrasonic can form an acoustic field between the workpiece and the ultrasonic radiator. The joints were welded by ultrasonic assisted under water wet welding process (U-FCAW) and underwater flux cored arc welding (FCAW), respectively. Observed change in properties was noticed as tensile, bending and hardness distribution. The results indicated that arc stability improved when ultrasonic was applied.

The amount of martensite (M) and upper bainite (BU) was decreased, while the granular bainite (BG) and acicular ferrite (AF) increased, after ultrasonic was introduced in welding. The tensile strength and the bending properties were improvised. The fracture occurrence of the welded joints during tensile testing was transferred from the joint to base metal, compared to FCAW. A 46% and 48% increase was found in the tensile strength of the upper and lower layers, respectively.[3]

The mechanism of ultrasonic welding for Al/Cu is still hard to explore. In this work, the microstructures of the ultrasonic welds between three layers of lithium-ion battery tabs (either Al or Cu) and bus bars were studied. the weld formation mechanism and failure modes were studied at microstructure level. The metal inter-mix is the main weld formation mechanism among Al tabs, while constrained surface deformation bonding is the main mechanism for Cu Cu or Al Cu. The weld failure is a combination of the interfacial debonding between the innermost tab (either Cu or Al) and the Cu bus bar and the Mode III through-thickness fracture of the tabs. This understanding and insight can be used to develop science-based design guidelines toward selecting the most appropriate materials (including heat treatment and coating), and welding configurations (such as layers of tabs), and welding process parameters. [4]

This research explores the joining between dissimilar alloys (magnesium alloy and titanium alloy) by ultrasonic spot welding. The tensile shear test shows that the joint strength increases with energy input. The fracture initiates inside magnesium alloy, indicating a high joining strength at the weld interface. Banded grain-refinement is found at the interface on the magnesium alloy side, neither transition layer nor inter-metallic compound layer is Identified though. The interfacial temperature exceeds the temperature range for liquefying magnesium alloy. The precipitated aluminum from the liquid-phase magnesium alloy plays a bridging role in ultrasonic welding of magnesium alloy to titanium alloy. [5]

A series of ultrasonic spot welding experiments with similar Mg alloy (AZ31B) were performed to deter-mine the process parameters and their effect on weld quality, including weld strength and fracture morphologies. Two dominant welding parameters including vibration amplitude and

welding time were evaluated independently to obtain good weld quality. A horn and an anvil tip surfaces were designed with pyramidal patterns to prevent slippage of lap-structured Mg alloy sheets among tool tips during ultrasonic spot welding process. The lap joint thinning was significant at higher vibration amplitudes and longer welding times and resulted in the variation of fracture types at the weld interface. Lap-shear tests on the ultrasonic spot welded Mg alloy lap joints yielded two fracture types: shear and pullout fracture. Metallographic examinations of the fracture surfaces provided insights on the fracture characteristics of the ultrasonic spot welded Mg alloys. Variations in the fracture morphologies were the results of the actual weld nugget development and closely related to weld quality. Higher weld strength was obtained at a low welding energy range of 100–140 J. [6]

### 3.0 Properties

#### 3.1 Thermal properties

Temperature at the centreline rised from 201 °C for 0.10 s to 345 °C for the optimum welding time of 0.30 s, and then to 440 °C at the longest welding time of 0.62s. Although , it was observed that the peak temperature dropped by 50–130 °C at the weld edge for different times. These variation confirmed that the heat exposure cycle was quite short and the weld components experienced fairly similar peak temperature. It was noted that the temperature increased extremely fast (350 °C within 0.22 s). For welding cycles (> 0.40 s) the steady state condition was rapidly achieved, which implied a balance between heat input and heat exhaustion in the thermo mechanically affected zone. The heating rate was seen to reduce with increasing the welding cycle. The cooling rate was also seen to be considerably high.[1]

#### 3.2 Mechanical performance

High power ultrasonic spot welding results in Surface damage due to tip penetration. This was verified for aluminium to aluminium joining processes. Fig. 1 demonstrates the average lap shear strength accompanied by fracture energy with increasing welding time under a 1.4 kN clamping force. With the increased welding time, the lap shear strength increased and approached the maximum level of 2.9 kN after 0.30 s, before reduction to 2.2 kN after 0.62 s. Fig. 1 b shows the fracture energies

of the joints that depict similar trends of lap shear strength.[1]

### 3.3 Grain structure

EBSID examinations commenced with the investigation of the as-received aluminium 6111-T4 sheet (Fig. 2). The microstructure was mainly equiaxed with an average grain size of  $\sim 22 \mu\text{m}$ , although some larger grains were randomly distributed throughout the aluminium sheet thickness (Fig. 2a). In addition, the grains had a largely random distribution of orientations (Fig. 2b).[1]

### 3.4 Joint performance: lap shear tensile testing and failure mode

The maximum tensile lap shear strengths of dissimilar USWed Al-to-AISI304 stainless steel and ASTM A36 steel joints as a function of welding energy are shown in Fig. 3.

The strength profiles for both joints showed a similar pattern, in which the lap shear strength increased with increasing energy input up to a peak value, then decreased with a further increase in the welding energy or welding time. In comparison with the lap shear strengths, the fracture energy of welded joints exhibited a larger scatter (Fig. 4), however showed a similar trend.

The optimum welding energy resulted in a peak value of the fracture energy followed by a decrease.

It can be seen that the Al-to-AISI304 stainless steel welds produced at a welding energy of 750J (in a welding time of 0.375s) gave a peak strength of  $\sim 87 \text{ MPa}$  ( $\sim 3.5 \text{ kN}$ ), which is higher than other dissimilar USW joints (with a similar clamping pressure), i.e. a maximum lap shear strength of  $3.2 \text{ kN}$  for aluminum AA6111-to-DC04 steel joints by Xu et al.,  $2.7 \text{ kN}$  for aluminum 6111-T4-to hard zinc-coated DX56-Z steel joints by Haddadi et al.,  $3.1 \text{ kN}$  for Al6111-to-hot-dipped Zn-coated steel, and  $2.7 \text{ kN}$  for Al6111-to-galvanized annealed steel by Haddadi et al. and  $0.6 \text{ kN}$  for A5052Al alloy-to-SS400 mild steel by Watanabe et al.

Compared to the Al-to-AISI304 stainless steel welds, the Al-to-ASTM A36 steel welds showed a slightly lower peak strength of  $\sim 83 \text{ MPa}$  ( $\sim 3.3 \text{ kN}$ ) in twice the time (in a 0.75s welding time) and twice the energy (1500J) in the lap shear tests and a much lower fracture energy (half of the Al-to-AISI304 stainless steel weld samples).[2]

### 3.5 Mechanical Properties

The mechanical properties of both FCAW welded joints (1#) and UFGAW welded joints (2#) were studied. The tensile tests of the welded joints and layered welded joints were performed at room temperature. The bending properties and the hardness were also tested. The effect of Ultrasonic on the tensile and bending properties was studied.[3]

#### 3.5.1. Bending testing

Three bending specimens of the welded joints from each welding method were tested to measure the bending ductility, at room temperature. Fig. 5 shows the angle of bending for the joints. According to the results, the maximum angle of the FCAW welded joints is  $21^\circ$ , which means bending ductility is very low. The formation of upper bainite (BU) and martensite (M) in welded metal are hardened phases. However, with the assistance of ultrasonic, granular bainite (BG) and acicular ferrite (AF) are the primary phases in the weld metal, which provide increased toughness and ductility. The angle of bending values was substantially increased. The bending angle can reach up to  $84^\circ$ . In conclusion, the welded joint ductility has been improved with the assistance of ultrasonic.

#### 3.5.2. Hardness distribution

Vickers hardness testing was carried out with a load of 3 N and a loading time of 10 s. Fig. 6 shows the results of hardness measurements. Decreased hardness values of the welded metal confirmed the above mentioned micro structural changes. It can be seen that the hardness of the HAZ was higher than that of the welded metal and the width of under layered HAZ is wider than the upper layered HAZ.

This is one of the reasons that the tensile strength of under layered specimens is lower than that of the upper layered specimens. The HAZ and welded metal hardness decreased with the assistance of ultrasonic. The maximum hardness values of HAZ is 450 HV at the under layered samples of FCAW due to the slag defects. The hardness values of the weld zone with the ultrasonic assistance are relatively lower due to the decrease in the amount of lath martensite (M) and Widmanstätten (W) structure while the amount of the granular bainite (BG) and acicular ferrite (AF) was increased. The results indicated that ultrasonic has a significant effect on the maximum hardness.

The hardness of the welded metal indicated that the application of ultrasonic decreases the hardness of the joints.[3]

### 3.6 Shear force

The shear load vs. the welding energy plot I shown in Fig. 7 at three different welding energy levels. The plot indicates that the peak shear force initially increases with the welding energy, and then starts to saturate at around 3200 J. Additional tests further discovered that the cccC lap shear strength actually decreases after certain energy levels (such as after 4000 J) due to the tab thinning and/or the weld spot circumferential fractures on the tabs. Note that the shear load is shown in a scaled form to protect proprietary data. The shear load v/s the welding energy plot is shown in Fig. 8 at three different energy levels. The plot indicates that the shear load initially increases with the welding energy, then reaches a plateau and the peak at around 800 J, after which sees an decrease at over-weld conditions due to tab thinning and the weld spot circumferential fractures on the tabs. Note that in Fig. 8, the shear load is in a scaled form to protect proprietary data.[4]

### 3.7 Micro structural analyses and mechanical tests of aaaC welds

- All three 0.2 mm Al layers were severely deformed, and the Al–Al interfaces were in wavy or curly. The amount of deformation decreased from outer to inner tabs. In particular, the Al inter-mixing is observed
- At the aaa|C interface, the copper surface remained almost straight/flat. This is no surprising since Al is much softer and ductile, and thus more deformable than the 0.9 mm Cu. As observed from fig 10.
- The grain size of the un-welded Al tab was about 50–67  $\mu\text{m}$  since there were about 3–4 grains through the 0.2 mm tab thickness(shown in the very left portion of Fig. 9 (top)). After ultrasonic welding, severe plastic deformation and material flow completely destroyed the original grain structure. Re-crystallization did not seem to occur because equiaxed new grains with well-defined grain boundaries were not observed ever in the most severely deformed region.
- The straight/flat boundaries between the three Al tab layers became highly wavy, curly, and

discontinued after welding. Metal flow, inter-mix and interlock were seen.

- The aaa|C interface, however, remained straight/flat. Therefore, the bonding mechanism between the innermost Al and the Cu layer was constrained surface deformation bonding. [4]

### 3.8 Temperature measurement

The temperature at the weld interface plays a significant role in ultrasonic spot welding process, so it is desirable to measure the interfacial temperature. The setup for temperature measurement is shown in Fig. 11(a). The temperature is actually measured at 0–0.5mm underneath the weld interface (probably impossible to measure the temperature exactly at the interface). The measured temperatures corresponding to different weld times are plotted in Fig. 11(b). It is observed that the peak temperature is 400 °C at welding time of 200 ms; however, when the welding time is increased to 700 and 800 ms, the corresponding peak temperature reaches 515 and 563 °C. It is well accepted that ultrasonic welding is a representative solid phase welding.

Nevertheless, numerous studies show that the weld interface may reach a relatively high temperature in welding light alloys. For example, the published measurement and simulation results show that the temperature at the weld interface can reach as high as 500 °C when welding aluminum alloy , 530 °C when welding magnesium alloy , 517 °C when welding Al/Ti-based alloys, and 440 °C when welding Al/Mg-based alloys. In the present experiment, the measured peak temperature 563 °C far exceeds the binary eutectic temperature of Mg\\Al (437 °C). Moreover, the liquid phase starting temperature of the magnesium alloy AZ31 measured by differential scanning calorimetry (DSC) is 559.2 °C according to Fig. 11(c). It is reasonable to conclude that in the present experiment the reaction temperature at the weld interface is sufficient for the magnesium alloy to produce a liquid phase. [5]

### 3.9 Failure loads and welding energy

Failure loads and welding energy inputs for various welding parameters adopted were analyzed and shown in Fig. 12. Shear fracture was the dominant fracture pattern on the weld interface at shorter welding time of 0.2 s even when vibration amplitude was varied from 31 mm to 35 mm (Fig. 12, open square).

It is categorized as “under weld” and is associated with welding energy input up to 90 J. At 0.4 s welding time and vibration amplitudes of 31 mm–35 mm, experiments against two tip mating configurations were conducted. Mating-tip Position 1 (Fig. 12, open circle), shows an increasing failure load before it slightly decreased upon reaching a welding energy input of 125 J. Shear fracture was also the governing fracture pattern at the weld interface, although some localized dimple-like ruptures were found on the fracture surfaces.[6]

**Fig 1 (a): Average Lap Shear Strength and (B) Failure Energy with Increasing Welding Time Under A 1.4kn Clamping Force.[1]**

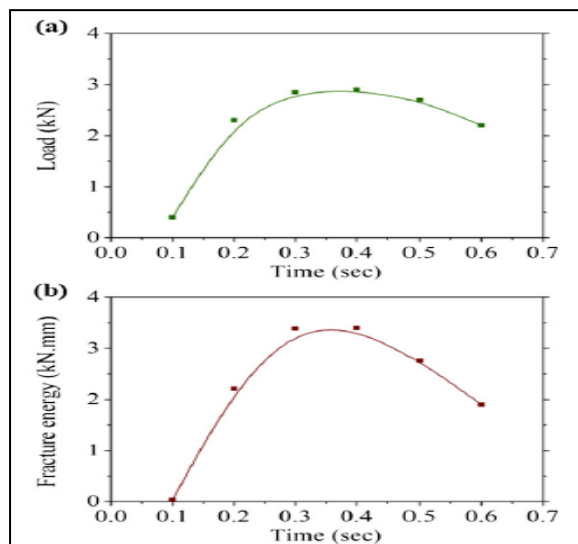


**Fig 2 (a): EBSD Euler Map of the Original Grain Structure, (b): Texture Component Map[1]**

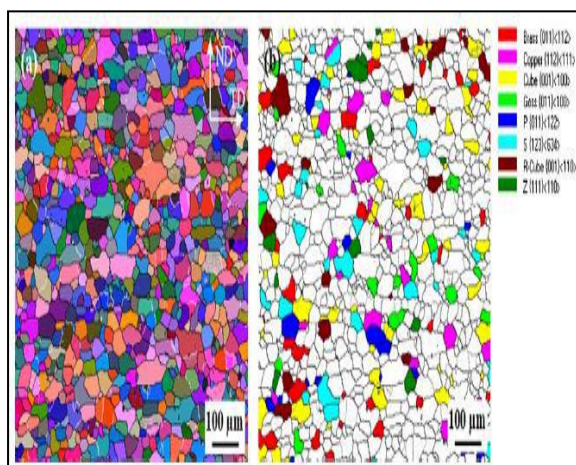


**Fig 3: Maximum Tensile Lap Shear Strength of Dissimilar Uswed al 6061-T6-To-Aisi304 Stainless Steel (A) and Al 6061-T6-to-Astm A36 Steel (B) Joints at Different Energy Inputs [2]**

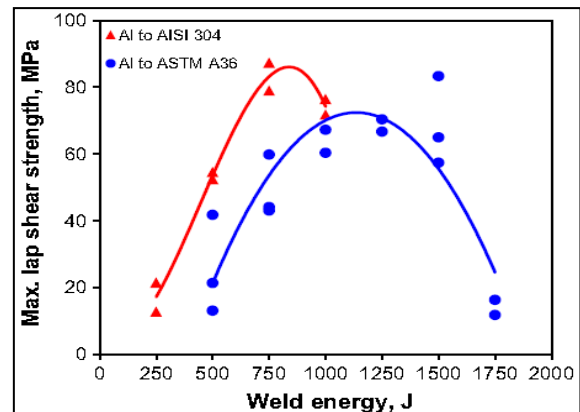


**Fig 4: Fracture Energy of Dissimilar Uswed al 6061-T6-to-Aisi 304 Stainless Steel (A) and al 6061-T6-to-Astm A36 Steel (B) Joints At Different Energy Inputs.[2]**

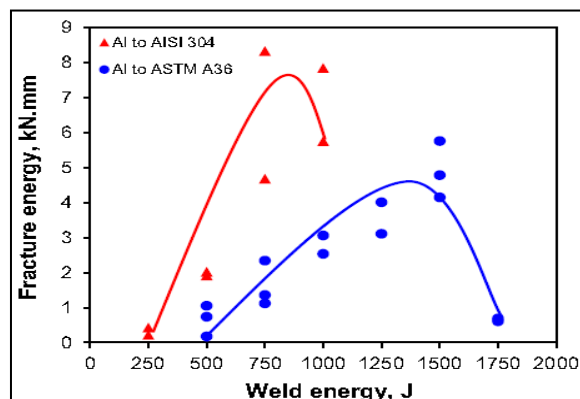


**Fig 5: Angle of Bending (1#) FCAW, (2#) U-FCAW.[3]**

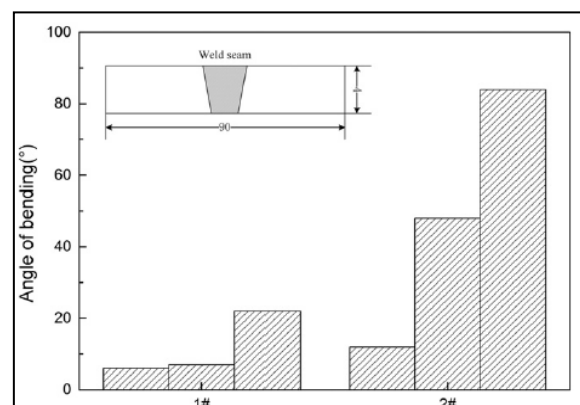




**Fig 6: Results of Hardness Measurements.[3]0.**

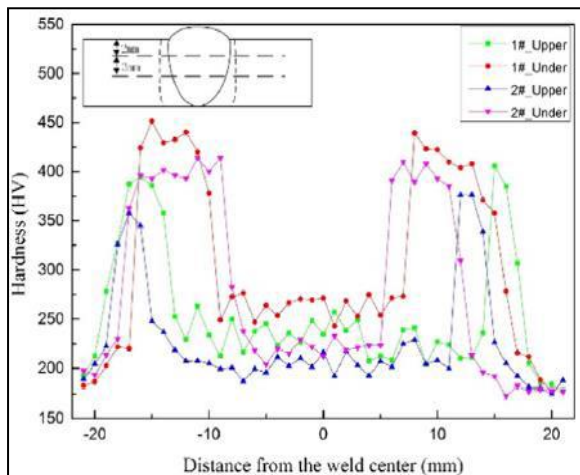


**Fig 7: The Shear Load (at the ccc|c interface) vs. Ultrasonic Welding Energy for Ccccwelds. [4]**

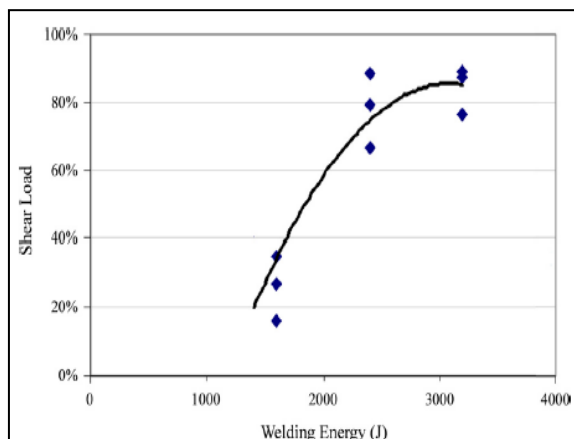


**Fig 8: The Shear Load (at the aaa|C interface) vs. Ultrasonic welding energy for aaacwelds.[4]**

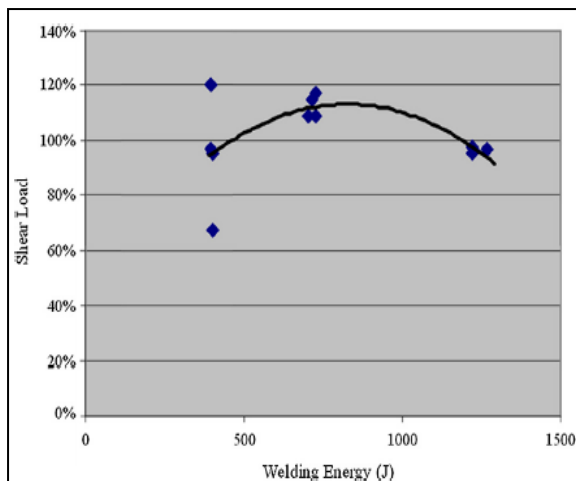


**Fig 9: Cross-Sectional Om View Of A Normal-Weld Specimen Sectioned Along The Axis For The Middle Weld Spot.[4]**

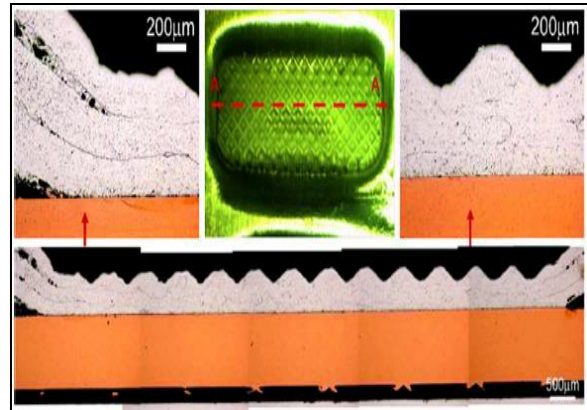


**Fig 10: Sectioned and Etched Al Tabs Interfaces, Observed by OM (1.8% HBF4 in distilled water; 20 vdc for 2 min; Sample at Anodic Pole; Olympus Omg 3; Polarizinglight Plus Sensitive Tint Lens). Cu Bus Bar is Not Shown.[4]**

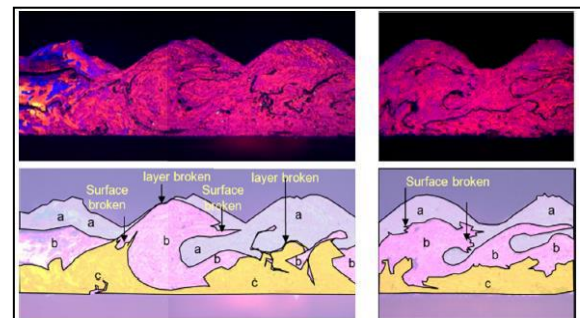


**Fig 11: Temperature at the Weld Interface: (a) Measurement Setup; (b) Temperature History Curve; (c) Differential Scanning Calorimetry Result of AZ31.[5]**

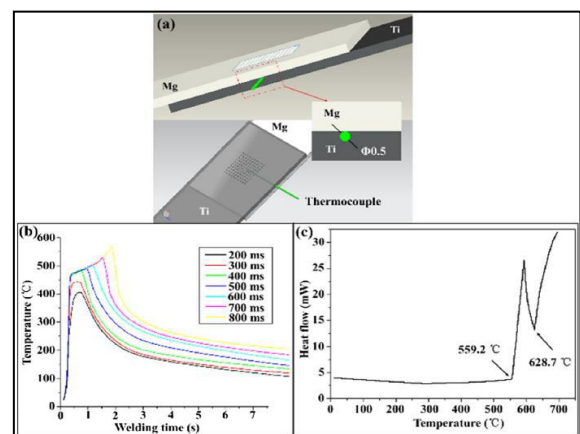
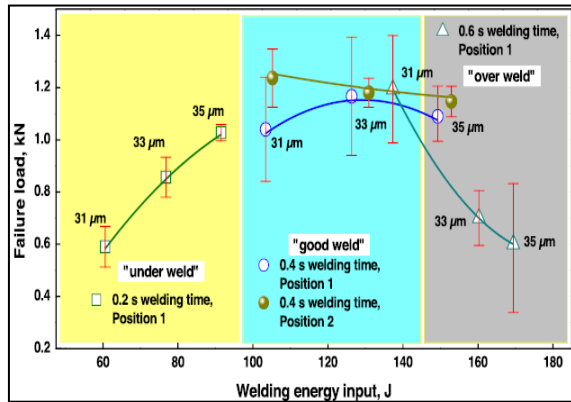


**Fig 12: Effects of Welding Parameters on The Failure Load and Welding Energy Input.[6]**



## 5.0 Conclusions

The purpose of this review study of Ultrasonic Welding, High Power Ultrasonic Spot Welding (HPUSW) and Ultrasonic assisted underwater wet welding is so to completely understand the properties and various aspects. In this review study it is completely confirmed that the ultrasonic spot welding is a promising solid state joining method for welding reinforced composites, carbon composites and other Metal Matrix Composites (MMC). Excellent weld quality and mechanical properties can be achieved within micro-seconds. For smaller time weld interface smaller micro bonds are formed which increases with increases in time and deformation at the weld surface occurs eventually. Ultrasonic assisted wet welding is used to improve arc stability and enhance mechanical properties of weld.

## References

- [1] Farid Haddadi, Dimitrios Tsivoulas. Grain structure, texture and mechanical property evolution of Automotive aluminium sheet during high power ultrasonic welding, 118, 2016, 340–35.
- [2] FAMirza, AMacwan, SD Bhole, DLChen, XG Chen. Effect of welding energy on microstructure and strength of ultrasonic spot welded dissimilar joints of aluminum to steel sheets, 668, 2016, 73–85.
- [3] QJ Sun, WQ Cheng, YB Liu, JF Wang, CW Cai, JC Feng. Microstructure and mechanical properties of ultrasonic assisted underwater wet welding joints, 103, 2016, 63–70.
- [4] Xin Wu, Teng Liu and Wayne Cai. Microstructure, welding mechanism, and failure of Al/Cu ultrasonic welds, 20, 2015, 515–524.
- [5] Daxin Ren, Kunmin Zhao, Min Pan, Ying Chang, Song Gang and Dewang Zhao, Ultrasonic spot welding of magnesium alloy to titanium alloy, 126, 2017, 58–62.
- [6] Michael de Leon and Hyung-Seop Shin, Weldability assessment of Mg alloy (AZ31B) sheets by an ultrasonicspot welding method, 243, 2017, 1–8.